

## ACCELERATING MULTIGRID OPTIMIZATION VIA SESOP\*

TAO HONG, IRAD YAVNEH AND MICHAEL ZIBULEVSKY

**Abstract.** A merger of two optimization frameworks is introduced: SEquential Subspace OPTimization (SESOP) with the MultiGrid (MG) optimization. At each iteration of the combined algorithm, search directions implied by the coarse-grid correction process of MG are added to the low dimensional search-spaces of SESOP, which include the (preconditioned) gradient and search directions involving the previous iterates (so-called history). The resulting accelerated technique is called SESOP-MG. The asymptotic convergence rate of the two-level version of SESOP-MG (dubbed SESOP-TG) is studied via Fourier mode analysis for linear problems (i.e., optimization of quadratic functionals). Numerical tests on linear and nonlinear problems demonstrate the effectiveness of the approach.

**Key words.** SESOP, acceleration, linear and nonlinear multigrid, history, linear and nonlinear large-scale problems

**AMS subject classifications.** 65N55, 65N22, 65H10

**1. Introduction.** MultiGrid (MG) methods are widely considered as a highly efficient approach for solving elliptic partial differential equations (PDEs) and systems, as well as other problems which can be effectively represented on a hierarchy of grids or levels. However, it is not always easy to design efficient MG methods for difficult problems, and therefore MG methods are often used in combination with acceleration techniques (e.g., [1]). Basically, there are two challenges in developing MG algorithms: choosing a cheap and effective smoother, often called Relaxation, and the design of a useful coarse-grid problem, whose solution yields a good coarse-grid correction. Imperfect choices of the latter often yields a deterioration of the convergence rates when many levels are used in the MG hierarchy, and the MG algorithm is not robust.

In this manuscript we study MG in an optimization framework and seek robust solution methods by merging this approach with so-called SEquential Subspace OPTimization (SESOP) [18] to obtain a robust solver. SESOP belongs to a general framework for addressing large-scale optimization problems, as described in the next section. The combined framework is called SESOP-MG, and its two-level version is named SESOP-TG. We analyze the convergence rate of SESOP-TG via local Fourier analysis (LFA) [2, 14] for quadratic optimization problems, and thus quantify the acceleration due to SESOP by means of the so-called  $h$ -ellipticity measure. Numerical experiments demonstrate the relevance of the theoretical analysis and the effectiveness of our novel scheme for addressing linear and nonlinear problems.

The rest of the paper is organized as follows. The standard MG and SESOP algorithms are briefly described in section 2. We then introduce the novel SESOP-MG scheme, and apply LFA to predict the SESOP-TG behavior for quadratic problems in section 3. Numerical results are shown in section 4 to demonstrate the effectiveness of SESOP-MG for solving linear and nonlinear problems. Conclusions are given in section 5.

We adopt the following notation throughout this paper. In the two-grid case, we use superscripts  $h$  and  $H$  to denote the fine and coarse grid. We assume  $H = 2h$ , although more aggressive coarsening may also be considered. Specifically,  $f^h(\mathbf{x}^h)$  and

---

\*Submitted to the editors DATE.

**Funding:** This work was funded by \*\*\*\*

$f^H(\mathbf{x}^H)$  denote the fine and coarse functions, respectively. The terms  $\nabla f^h(\mathbf{x}^h)$  and  $\nabla f^H(\mathbf{x}^H)$  are used to define the gradients of  $f^h(\mathbf{x}^h)$  and  $f^H(\mathbf{x}^H)$ , respectively. In the single-grid case, we may omit the superscript  $h$ . In the MG case, we use  $f_{l,k}(\mathbf{x}_{l,k})$  to denote the  $l$ -level function at  $k$ th iteration where  $l = 1$  denotes the finest level and  $l = L$  the coarsest one, assuming a total of  $L$  levels. If the vector  $\mathbf{x}$  has only one subscript, e.g.,  $\mathbf{x}_l$ , the subscript  $l$  either refers to the variables at  $l$ th level or  $l$ th iteration, and thus  $\mathbf{x}_l$  itself is a vector, or it refers to the  $l$ th element of the vector  $\mathbf{x}$ . If the subscript  $l$  in  $\mathbf{x}_l$  is used to denote the  $l$ th iteration, we use  $\mathbf{x}_l(k)$  to represent the  $k$ th element in  $\mathbf{x}_l$ . When the use of subscript is not clear from the context, the specific meaning is clarified. In particular, if  $\mathbf{A}$  is a matrix, we use  $\mathbf{a}_l$  and  $\mathbf{a}_{l,k}$  to denote its  $l$ th column and  $(l, k)$ th element. Note that we use a boldface font to denote vectors and matrices. We use  $\mathbf{\tau}$  for the transpose operator.

**2. Preliminaries.** In this section we briefly describe MG and SESOP—the building-blocks of SESOP-MG, which are merged in the next section.

**2.1. MultiGrid (MG).** MG methods are considered to be amongst of the most efficient numerical ways for solving large-scale systems of equations (linear and non-linear) arising from the discretization of elliptic partial differential equations (PDEs) [1, 3, 13, 17]. These types of methods can be viewed as an acceleration of simple and inexpensive traditional iterative methods based on local relaxation, e.g., Jacobi or Gauss-Seidel. Such methods are typically very efficient at reducing errors that are oscillatory with respect to the grid, but inefficient for errors that are relatively “smooth”, that is, undergo little change over the span of a few mesh intervals. The main idea in MG methods is to project the error obtained after applying a few iterations of local relaxation onto a coarser grid. This yields two advantages. First, the resulting coarse-grid system is smaller, hence cheaper to solve. Second, part of the slowly converging smooth error on a finer grid becomes relatively more oscillatory on the coarser grid, and therefore can be treated more efficiently by a local relaxation method. Thus, the coarse-grid problem is treated recursively, by applying relaxation and projecting to a still coarser grid resulting in a multi-level version. Once the coarse-grid problem is solved approximately, its solution is prolonged and added to the fine-grid approximation—this is called coarse-grid correction.

In preparation towards merging MG with SESOP, we cast our problem in variational form as a nested hierarchy of optimization problems (see, e.g., [6, 9]). We adopt the common MG notation, where it is assumed that the function we wish to minimize is defined on a grid with nominal mesh-size  $h$  and is denoted  $f^h$ . For simplicity, we consider the two-level (or two-grid) framework, with the coarse-grid mesh-size denoted by  $H$ , and discuss the extension to multi-levels later.

Consider the following unconstrained problem defined on the fine-grid:

$$(2.1) \quad \mathbf{x}_*^h = \underset{\mathbf{x}^h \in \mathfrak{R}^N}{\operatorname{argmin}} f^h(\mathbf{x}^h),$$

where  $f^h(\mathbf{x}^h) : \mathfrak{R}^N \rightarrow \mathfrak{R}$  is a differentiable function and the solution set of (2.1) is not empty. Let  $\mathbf{x}_k^h$  denote our approximation to the fine-grid solution  $\mathbf{x}_*^h$  after the  $k$ th iteration. Assume that we have defined a *restriction* operator  $\mathbf{I}_h^H : \mathfrak{R}^N \rightarrow \mathfrak{R}^{N_c}$ , and a *prolongation* operator  $\mathbf{I}_H^h : \mathfrak{R}^{N_c} \rightarrow \mathfrak{R}^N$ , where  $N_c$  is the size of the coarse grid. Furthermore, let  $\mathbf{x}_k^H$  denote a coarse-grid approximation to  $\mathbf{x}_k^h$  (for example, we may use  $\mathbf{x}_k^H = \mathbf{I}_h^H \mathbf{x}_k^h$ , but other choices may be used as well). The coarse-grid problem is

then defined as follows:

$$(2.2) \quad \mathbf{x}_*^H = \operatorname{argmin}_{\mathbf{x}^H \in \Re^{N_c}} f^H(\mathbf{x}^H) - \mathbf{v}_k^T \mathbf{x}^H,$$

where  $f^H$  is the coarse approximation of  $f^h$ , and  $\mathbf{v}_k = \nabla f^H(\mathbf{x}_k^H) - \mathbf{I}_h^H \nabla f^h(\mathbf{x}_k^h)$ . The correction term  $\mathbf{v}_k$  is used to enforce the same first-order optimality condition [9] on the fine and coarse levels. After solving (2.2) (by some methods), the coarse-grid correction direction is given by

$$(2.3) \quad \mathbf{d}_k^h = \mathbf{I}_H^h \mathbf{d}_k^H = \mathbf{I}_H^h (\mathbf{x}_*^H - \mathbf{x}_k^H).$$

Finally, the coarse-grid correction is interpolated and added to the current fine-grid approximation:

$$(2.4) \quad \mathbf{x}_{k+1}^h = \mathbf{x}_k^h + \mathbf{d}_k^h.$$

This may be followed by additional relaxation steps.

**2.2. SEquential Subspace OPtimization (SESOP).** We are concerned with the solution of smooth large-scale unconstrained problems

$$(2.5) \quad \min_{\mathbf{x} \in \Re^N} f(\mathbf{x}).$$

The SESOP approach [8, 4, 19, 18] is an established framework for solving (2.5) by sequential optimization over affine subspaces  $\mathcal{M}_k$ , spanned by the current descent direction (typically preconditioned gradient) and  $\Pi$  previous propagation directions of the method. If  $f(\mathbf{x})$  is convex, SESOP yields the optimal worst-case convergence rate of  $O(\frac{1}{k^2})$  [8], while achieving efficiency of the quadratic Conjugate-Gradient (CG) method when the problem is close to quadratic or in the vicinity of the solution.

The affine subspace at the iteration  $k$  is defined by

$$\mathcal{M}_k = \{\mathbf{x}_k + \mathbf{P}_k \boldsymbol{\alpha} : \boldsymbol{\alpha} \in \Re^{\Pi+1}\},$$

where  $\mathbf{x}_k$  is  $k$ th iterate, the matrix  $\mathbf{P}_k$  contains spanning directions in its columns, the preconditioned gradient  $\Phi \nabla f(\mathbf{x}_k)$  and  $\Pi$  last steps  $\mathbf{d}_i = \mathbf{x}_i - \mathbf{x}_{i-1}$ ,

$$(2.6) \quad \mathbf{P}_k = [\Phi \nabla f(\mathbf{x}_k), \mathbf{d}_k, \mathbf{d}_{k-1}, \dots, \mathbf{d}_{k-\Pi+1}], \quad \Pi \geq 0.$$

The new iterate  $\mathbf{x}_{k+1}$  is obtained via optimization of  $f(\cdot)$  over the current subspace  $\mathcal{M}_k$ ,

$$(2.7) \quad \begin{aligned} \tilde{\boldsymbol{\alpha}} &= \operatorname{argmin}_{\boldsymbol{\alpha} \in \Re^{\Pi+1}} f(\mathbf{x}_k + \mathbf{P}_k \boldsymbol{\alpha}), \\ \mathbf{x}_{k+1} &= \mathbf{x}_k + \mathbf{P}_k \tilde{\boldsymbol{\alpha}}. \end{aligned}$$

By keeping the dimension of  $\boldsymbol{\alpha}$  low, (2.7) can be solved efficiently with a Newton-type method. SESOP is relatively efficient if the following two conditions are satisfied:

- The objective function can be represented as  $\psi(\mathbf{A}\mathbf{x})$ .
- Evaluation of  $\psi(\cdot)$  is cheap, but calculating  $\mathbf{A}\mathbf{x}$  is expensive.

In this case, storing  $\mathbf{A}\mathbf{P}_k$  and  $\mathbf{A}\mathbf{x}_k$ , we can avoid re-computation of  $\mathbf{A}\mathbf{x}_k$  during the subspace minimization. A typical class of problems of this type is the well-known  $\ell_1 - \ell_2$  optimization [19].

SESOP can yield faster convergence if more efficient descent directions are added to the subspace  $\mathcal{M}_k$ . This may include cumulative or parallel coordinate descent step, separable surrogate function or expectation-maximization step, Newton-type steps and some others [4, 19, 18]. In this work we suggest adding the coarse-grid correction direction, obtained through the MG framework.

**3. Merging SESOP with Multigrid.** The main idea we are pursuing in this manuscript is merging the SESOP optimization framework with MG by enriching the SESOP subspace  $\mathbf{P}_k$  with one or more directions implied by the coarse-grid correction. We expect that robust and efficient algorithms for large-scale optimization problems can be obtained through such a merger in cases where a multi-scale hierarchy can be usefully defined. The numerical experiments on linear and nonlinear problems demonstrate the potential advantage of this approach, see [section 4](#). Moreover, the convergence rate analysis of SESOP-TG for the quadratic case in [subsection 3.1](#) also indicates the potential merits of merging SESOP with MG.

We begin this section by introducing a two-grid version of our scheme first, SESOP-TG, and later extend it to a multi-level version, SESOP-MG. At its basic form, the idea is to add the coarse correction  $\mathbf{d}_k^h$  of [\(2.3\)](#) into the affine subspace  $\mathbf{P}_k$ , obtaining the augmented subspace  $\bar{\mathbf{P}}_k = [\mathbf{d}_k^h \ \mathbf{P}_k]$ . We then replace  $\mathbf{P}_k$  by  $\bar{\mathbf{P}}_k$  in [\(2.7\)](#) and compute the locally optimal  $\boldsymbol{\alpha}$  to obtain the next iterate,  $\mathbf{x}_{k+1}$ . Our intention is to combine the efficiency of MG that results from fast reduction of large-scale error by the coarse-grid correction, with the robustness of SESOP that results from the local optimization over the subspace. That is, even in difficult cases where the coarse-grid correction is poor, the algorithm should still converge at least as fast as standard SESOP, because an inefficient direction simply results in small (or conceivably even negative) weighting. The SESOP-TG is presented in [Algorithm 3.1](#). Note that we add two steps to the usual SESOP algorithm, the pre- and post-relaxation steps 2 and 7 in [Algorithm 3.1](#), commonly applied in MG algorithms. This allows us to advance the solution with low computational expense whenever the coarse-grid direction is highly inefficient.

---

**Algorithm 3.1** SESOP-TG

---

**Initialization:** Initial value  $\mathbf{x}_1^h$ , the number of iterations  $Iter_{max}$ , the size of subspace  $\Pi \geq 0$  and  $v_1, v_2$  denote the number of pre- and post-relaxation.

**Output:** Final Solution:  $\mathbf{x}_*^h$

- 1: **for**  $k = 1 : Iter_{max}$  **do**
- 2:    $\mathbf{x}_k^h \leftarrow Relaxation(\mathbf{x}_k^h, v_1)$
- 3:   Calculate the gradient:  $\nabla f^h(\mathbf{x}_k^h)$  and formulate the subspace  $\mathbf{P}_k \leftarrow [\Phi \nabla f^h(\mathbf{x}_k^h) \ \mathbf{x}_k^h - \mathbf{x}_{k-1}^h \ \cdots \ \mathbf{x}_{k-\Pi+1}^h - \mathbf{x}_{k-\Pi}^h]$
- 4:   Solving the coarse problem [\(2.2\)](#) results in  $\mathbf{x}_*^H$ .
- 5:   Formulate the coarse correction  $\mathbf{d}_k^h = \mathbf{I}_H^h (\mathbf{x}_*^H - \mathbf{I}_h^H \mathbf{x}_k^h)$  and renew the subspace as  $\bar{\mathbf{P}}_k \leftarrow [\mathbf{d}_k^h \ \mathbf{P}_k]$ .
- 6:   Address [\(2.7\)](#) on  $\bar{\mathbf{P}}_k$  and then  $\mathbf{x}_{k+1}^h \leftarrow \mathbf{x}_k^h + \bar{\mathbf{P}}_k \boldsymbol{\alpha}_k$ .
- 7:    $\mathbf{x}_{k+1}^h \leftarrow Relaxation(\mathbf{x}_{k+1}^h, v_2)$
- 8: **end for**
- 9:  $\mathbf{x}_*^h \leftarrow \mathbf{x}_{Iter_{max}+1}^h$
- 10: **return**

---

**3.1. Convergence Rate Analysis of SESOP-TG for Quadratic Problems.** To gain insight, we analyze our proposed algorithm for quadratic optimization problems that are equivalent to the solution of linear systems. We first derive a rather general formulation for the case of SESOP-TG with a single history ( $\Pi = 1$ ). Then, we explore further under certain simplifying assumptions.

Consider the linear system

$$(3.1) \quad \mathbf{A}\mathbf{x} = \mathbf{b},$$

where  $\mathbf{A} \in \Re^{N \times N}$  is a symmetric positive-definite (SPD) matrix. Evidently, solving (3.1) is equivalent to the following quadratic minimization problem:

$$(3.2) \quad \mathbf{x}^* = \underset{\mathbf{x} \in \Re^N}{\operatorname{argmin}} f(\mathbf{x}) \triangleq \frac{1}{2} \mathbf{x}^T \mathbf{A} \mathbf{x} - \mathbf{b}^T \mathbf{x}.$$

Given iterates  $\mathbf{x}_{k-1}$  and  $\mathbf{x}_{k-2}$ , the next iterate produced by SESOP-TG with a single history is given by

$$(3.3) \quad \mathbf{x}_k = \mathbf{x}_{k-1} + c_1(\mathbf{x}_{k-1} - \mathbf{x}_{k-2}) + c_2 \Phi(\mathbf{b} - \mathbf{A}\mathbf{x}_{k-1}) + c_3 \mathbf{I}_H^h \mathbf{A}_H^{-1} \mathbf{I}_h^H (\mathbf{b} - \mathbf{A}\mathbf{x}_{k-1}),$$

where  $c_1, c_2, c_3$  are the locally optimal weights associated with the three directions comprising  $\mathbf{P}_k$ :  $c_1$  multiplies the so-called history, that is, the difference between the last two iterates;  $c_2$  multiplies the preconditioned gradient;  $c_3$  multiplies the coarse-grid correction direction  $\mathbf{d}_{k-1}^h$ . Here,  $\mathbf{A}_H$  represents the coarse-grid matrix approximating  $\mathbf{A}$ , which is most commonly defined by the Galerkin formula,  $\mathbf{A}_H = \mathbf{I}_h^H \mathbf{A} \mathbf{I}_H^h$ , or simply by rediscretization on the coarse-grid in the case where  $\mathbf{A}$  is the discretization of an elliptic partial differential equation on the fine-grid. Subtracting  $\mathbf{x}^*$  from both sides of (3.3), and denoting the error by  $\mathbf{e}_k = \mathbf{x}^* - \mathbf{x}_k$ , we get

$$(3.4) \quad \mathbf{e}_k = \mathbf{e}_{k-1} + c_1(\mathbf{e}_{k-1} - \mathbf{e}_{k-2}) - c_2 \Phi \mathbf{A} \mathbf{e}_{k-1} - c_3 \mathbf{I}_H^h \mathbf{A}_H^{-1} \mathbf{I}_h^H \mathbf{A} \mathbf{e}_{k-1}.$$

Rearranging (3.4) yields

$$(3.5) \quad \mathbf{e}_k = \mathbf{\Gamma} \mathbf{e}_{k-1} - c_1 \mathbf{e}_{k-2},$$

where

$$(3.6) \quad \mathbf{\Gamma} = (1 + c_1) \mathbf{I} - (c_2 \Phi + c_3 \mathbf{I}_H^h \mathbf{A}_H^{-1} \mathbf{I}_h^H) \mathbf{A},$$

and  $\mathbf{I}$  denotes the identity matrix. Define the vector  $\mathbf{E}_k = \begin{bmatrix} \mathbf{e}_k \\ \mathbf{e}_{k-1} \end{bmatrix}$ . Then, (3.5) implies the following relation:

$$(3.7) \quad \mathbf{E}_k = \mathbf{\Upsilon} \mathbf{E}_{k-1}, \quad \mathbf{\Upsilon} \triangleq \begin{bmatrix} \mathbf{\Gamma} & -c_1 \mathbf{I} \\ \mathbf{I} & \mathbf{0} \end{bmatrix}.$$

To analyze the convergence factor of SESOP-TG, we will continue under the assumption that the coefficients  $c_j$ ,  $j = 1, \dots, 3$  do not change from iteration to iteration, and we will search for the optimal fixed coefficients. In practice, the coefficients do vary but we will verify numerically that the analysis is nonetheless very relevant inasmuch as the SESOP-TG convergence history curve oscillates around the optimal fixed- $c_j$  curve, so there is a near-match in an average sense. For fixed  $c_j$ , the asymptotic convergence factor of the SESOP-TG iteration is determined by the spectral radius of  $\mathbf{\Upsilon}$ . Let  $r$  denote an eigenvalue of  $\mathbf{\Upsilon}$  with eigenvector  $\mathbf{v} = [\mathbf{v}_1, \mathbf{v}_2]^T$ :

$$\begin{bmatrix} \mathbf{\Gamma} & -c_1 \mathbf{I} \\ \mathbf{I} & \mathbf{0} \end{bmatrix} \begin{bmatrix} \mathbf{v}_1 \\ \mathbf{v}_2 \end{bmatrix} = r \begin{bmatrix} \mathbf{v}_1 \\ \mathbf{v}_2 \end{bmatrix}.$$

Hence,  $\mathbf{v}_1 = r\mathbf{v}_2$  and  $\mathbf{\Gamma v}_1 - c_1\mathbf{v}_2 = r\mathbf{v}_1$ . This yields

$$\mathbf{\Gamma v}_1 = \left( r + \frac{c_1}{r} \right) \mathbf{v}_1.$$

Thus,  $\mathbf{v}_1$  is an eigenvector of  $\mathbf{\Gamma}$  with eigenvalue  $b = r + \frac{c_1}{r}$ . This leads to the following quadratic equation:

$$r^2 - br + c_1 = 0,$$

with solutions

$$r_{1,2} = \frac{1}{2} \left( b \pm \sqrt{b^2 - 4c_1} \right).$$

The asymptotic convergence factor is given by the spectral radius of  $\mathbf{\Upsilon}$ ,

$$(3.8) \quad \rho(\mathbf{\Upsilon}) = \max_b \left| \frac{1}{2} \left( b \pm \sqrt{b^2 - 4c_1} \right) \right|,$$

where  $b$  runs over the eigenvalues of  $\mathbf{\Gamma}$ . For the remainder of our analysis we focus on the case where the eigenvalues  $b$  of  $\mathbf{\Gamma}$  are all real.

**3.1.1. The case of real  $\mathbf{b}$ .** In many practical cases, the eigenvalues of  $\mathbf{\Gamma}$  are all real, which simplifies the analysis and yields insight. We focus next on a common situation where this is indeed the case.

LEMMA 3.1. *Assume:*

1. *The prolongation has full column-rank and the restriction is the transpose of the prolongation:  $I_h^H = (I_H^h)^\mathcal{T}$  (optionally up to a positive multiplicative constant).*
2. *The coarse-grid operator  $\mathbf{A}_H$  is SPD.*
3. *The preconditioner  $\mathbf{\Phi}$  is SPD.*

*Then the eigenvalues of  $\mathbf{\Gamma} = (1 + c_1)\mathbf{I} - (c_2\mathbf{\Phi} + c_3\mathbf{I}_H^h\mathbf{A}_H^{-1}\mathbf{I}_h^H)\mathbf{A}$  are all real.*

*Proof.* Because  $\mathbf{A}$  is SPD, there exists a SPD matrix  $\mathbf{S} = \sqrt{\mathbf{A}}$  such that  $\mathbf{S}^2 = \mathbf{A}$ . The matrix

$$\mathbf{S}\mathbf{\Gamma}\mathbf{S}^{-1} = (1 + c_1)\mathbf{I} - \mathbf{S}(c_2\mathbf{\Phi} + c_3\mathbf{I}_H^h\mathbf{A}_H^{-1}\mathbf{I}_h^H)\mathbf{S}$$

is similar to  $\mathbf{\Gamma}$  so they have the same eigenvalues. Moreover,  $\mathbf{S}\mathbf{\Gamma}\mathbf{S}^{-1}$  is evidently symmetric, so its eigenvalues are all real.  $\square$

The first two assumptions of this lemma are satisfied very commonly, including of course both the case where  $\mathbf{A}_H$  is defined by rediscretization on the coarse grid and the case of Galerkin coarsening,  $\mathbf{A}_H = (\mathbf{I}_H^h)^\mathcal{T} \mathbf{A} \mathbf{I}_h^H$ . The preconditioner  $\mathbf{\Phi}$  is SPD for commonly used MG relaxation methods, including Richardson (where  $\mathbf{\Phi}$  is the identity matrix), Jacobi (where  $\mathbf{\Phi}$  is the inverse of the diagonal of  $\mathbf{A}$ ), and symmetric Gauss-Seidel.

We next adopt the change of variables  $c_{23} = c_2 + c_3$ ,  $\alpha = c_2/c_{23}$ . This yields

$$(3.9) \quad \mathbf{\Gamma} = (1 + c_1)\mathbf{I} - c_{23}\mathbf{W}_\alpha,$$

with

$$(3.10) \quad \mathbf{W}_\alpha = (\alpha\mathbf{\Phi} + (1 - \alpha)\mathbf{I}_H^h\mathbf{A}_H^{-1}\mathbf{I}_h^H) \mathbf{A}.$$

LEMMA 3.2. *The eigenvalues of  $\mathbf{W}_\alpha$  are real and positive for any  $\alpha \in (0, 1]$ .*

*Proof.* This follows from the fact that  $\Phi$  is SPD, and  $I_H^h \mathbf{A}_H^{-1} I_h^H$  is symmetric positive semi-definite. Hence,  $\mathbf{W}_\alpha$  is the product of two SPD matrices and  $\mathbf{S} \mathbf{W}_\alpha \mathbf{S}^{-1}$ , where  $\mathbf{S} = \sqrt{\mathbf{A}}$  as above, is SPD.  $\square$

We henceforth denote the eigenvalues of  $\mathbf{W}_\alpha$  by  $\lambda$ , and assume  $\alpha \in (0, 1]$  (that is,  $c_2$  and  $c_3$  are of the same sign), so the  $\lambda$ 's are all real and positive. We then proceed by fixing  $\alpha$  and optimizing  $c_1$  and  $c_{23}$ . That is, we seek  $c_1$  and  $c_{23}$  which minimize the spectral radius of  $\mathbf{T}$ . Under our assumptions, we have  $b \equiv b(c_1, c_{23}, \lambda) = 1 + c_1 - c_{23}\lambda$ , and the worst-case convergence factor is given by:

$$(3.11) \quad \bar{r}(c_1, c_{23}) \triangleq \rho(\mathbf{T}) = \max_{\lambda} |r(c_1, c_{23}, \lambda)|,$$

where  $r = \frac{1}{2} (b \pm \sqrt{b^2 - 4c_1})$ . Per each  $\lambda$ , this quadratic equation obviously has two solutions. Let us denote the absolute value of the solution whose absolute value is the larger of the two by  $\hat{r}$ . Then we can write (3.11) as follows:

$$(3.12) \quad \bar{r}(c_1, c_{23}) = \max_{\lambda} \hat{r}(c_1, c_{23}, \lambda) \triangleq \frac{1}{2} \left| b + \operatorname{sgn}(b) \sqrt{b^2 - 4c_1} \right|.$$

Here,  $\operatorname{sgn}(\cdot)$  is equal to 1 for non-negative arguments and -1 for negative arguments. Our parameter optimization problem is now defined by

$$(\bar{c}_1, \bar{c}_{23}) = \operatorname{argmin}_{(c_1, c_{23})} \bar{r}(c_1, c_{23}).$$

**LEMMA 3.3.**  $\bar{r}(c_1, c_{23})$  depends only on the maximal and minimal eigenvalues of  $\mathbf{W}_\alpha$ , denoted by  $\lambda_{\max}$  and  $\lambda_{\min}$ , respectively.

*Proof.* Consider  $\hat{r}$  in (3.12) as a continuous function of a positive variable  $\lambda \in [\lambda_{\min}, \lambda_{\max}]$ , with fixed  $c_1$  and  $c_{23}$ :

$$\hat{r}(c_1, c_{23}, \lambda) = \frac{1}{2} \left| b(c_1, c_{23}, \lambda) + \operatorname{sgn}(b(c_1, c_{23}, \lambda)) \sqrt{b^2(c_1, c_{23}, \lambda) - 4c_1} \right|.$$

We distinguish between two regimes: (I):  $b^2 < 4c_1$  and (II):  $b^2 \geq 4c_1$ . In case (I), the square-root term is imaginary, and we simply get  $\hat{r} = \sqrt{c_1}$ . In case (II) the square-root term is real. Differentiating  $\hat{r}$  with respect to  $\lambda$  we then get

$$\frac{\partial \hat{r}}{\partial \lambda} = -\frac{c_{23}}{2} \operatorname{sgn}(b(c_1, c_{23}, \lambda)) \left[ 1 + \frac{|b(c_1, c_{23}, \lambda)|}{\sqrt{b^2(c_1, c_{23}, \lambda) - 4c_1}} \right]$$

We ignore the irrelevant choice  $c_{23} = 0$ , for which the method is obviously not convergent. Then, using  $b(c_1, c_{23}, \lambda) = c_{23} \left( \lambda - \frac{1+c_1}{c_{23}} \right)$ , we obtain

$$\frac{\partial \hat{r}}{\partial \lambda} = \frac{|c_{23}|}{2} \operatorname{sgn} \left( \lambda - \frac{1+c_1}{c_{23}} \right) \left[ 1 + \frac{|b(c_1, c_{23}, \lambda)|}{\sqrt{b^2(c_1, c_{23}, \lambda) - 4c_1}} \right].$$

We conclude that  $\hat{r}$  is evidently a symmetric function of  $\lambda - (1+c_1)/c_{23}$ , and it is furthermore convex, because its derivative is strictly negative for  $\lambda < (1+c_1)/c_{23}$  and positive for  $\lambda > (1+c_1)/c_{23}$ . It follows that, regardless of the sign of  $b^2 - 4c_1$  throughout the regime  $\lambda \in [\lambda_{\min}, \lambda_{\max}]$ , there exists no local maximum of  $\bar{r}$ . Hence,

$$(3.13) \quad \bar{r}(c_1, c_{23}) = \max(\hat{r}(c_1, c_{23}, \lambda_{\min}), \hat{r}(c_1, c_{23}, \lambda_{\max})).$$

This completes the proof.  $\square$

LEMMA 3.4. *For any fixed  $c_1$ ,  $\bar{r}(c_1, c_{23})$  is minimized with respect to  $c_{23}$  by choosing it such that  $b(c_1, c_{23}, \lambda_{\min}) = -b(c_1, c_{23}, \lambda_{\max})$ , and hence  $\hat{r}(c_1, c_{23}, \lambda_{\max}) = \hat{r}(c_1, c_{23}, \lambda_{\min})$ . The resulting optimal  $c_{23}$  is given by  $c_{23} = 2(1 + c_1)/(\lambda_{\max} + \lambda_{\min})$ .*

*Proof.* Considering now  $\hat{r}(c_1, c_{23}, \lambda)$  as a continuous function of a real variable  $c_{23}$ , with  $c_1$  and  $\lambda$  fixed, we can apply the same arguments as in the previous lemma to show that  $\hat{r}$  is a convex symmetric function of  $c_{23} - \frac{(1+c_1)}{\lambda}$ . Differentiating  $\hat{r}$  with respect to  $c_{23}$ , we simply exchange the roles of  $\lambda$  and  $c_{23}$ , obtaining

$$\frac{\partial \hat{r}}{\partial c_{23}} = \frac{|\lambda|}{2} \operatorname{sgn} \left( c_{23} - \frac{1 + c_1}{\lambda} \right) \left[ 1 + \frac{|b(c_1, c_{23}, \lambda)|}{\sqrt{b^2(c_1, c_{23}, \lambda) - 4c_1}} \right].$$

As in the previous lemma, it follows that the meeting point of  $\hat{r}(c_1, c_{23}, \lambda_{\max})$  and  $\hat{r}(c_1, c_{23}, \lambda_{\min})$ , which lies between  $c_{23} = (1 + c_1)/\lambda_{\max}$  and  $c_{23} = (1 + c_1)/\lambda_{\min}$ , is where  $\hat{r}$  is minimized with respect to  $c_{23}$ : for larger  $c_{23}$ ,  $\hat{r}(c_1, c_{23}, \lambda_{\max})$  is at least as large as at this point, while for smaller  $c_{23}$ ,  $\hat{r}(c_1, c_{23}, \lambda_{\min})$  is at least as large. At the meeting point

$$1 + c_1 - c_{23}\lambda_{\max} = -(1 + c_1 - c_{23}\lambda_{\min}),$$

yielding

$$(3.14) \quad c_{23} = \frac{2(1 + c_1)}{\lambda_{\min} + \lambda_{\max}}.$$

This completes the proof.  $\square$

Plugging the optimal  $c_{23}$  into (3.12) yields

$$(3.15) \quad \bar{r} = \min_{c_1} \frac{1}{2} \left| \mu(1 + c_1) + \sqrt{\mu^2(1 + c_1)^2 - 4c_1} \right|,$$

with

$$\mu = \frac{\kappa - 1}{\kappa + 1},$$

where  $\kappa = \frac{\lambda_{\max}}{\lambda_{\min}}$  is the condition number of  $\mathbf{W}_\alpha$ . In Lemma 3.5, we determine the optimal  $c_1$ , which minimizes  $\bar{r}$  in (3.15). We assume  $\kappa$  to be strictly greater than 1, so  $\mu \in (0, 1)$ . That is, we omit the trivial case  $\kappa = 1$ , for which convergence occurs in a single iteration with  $c_1 = 0$ .

LEMMA 3.5. *The spectral radius  $\bar{r}$  of the iteration matrix is minimized with respect to  $c_1$  by choosing it such that the square-root term in (3.15) vanishes:  $\mu^2(1 + c_1)^2 - 4c_1 = 0$ . This yields*

$$(3.16) \quad c_1^\pm = \frac{2}{\mu^2} - 1 \pm \frac{2}{\mu^2} \sqrt{1 - \mu^2},$$

and the minimizer  $c_1^-$  is the solution with the minus sign before the square-root term.

*Proof.* Note first that  $c_1^\pm$  are always real, because  $\mu \in (0, 1)$ , and positive, because

$$c_1^- = \frac{2}{\mu^2} - 1 - \frac{2}{\mu^2} \sqrt{1 - \mu^2} = \sqrt{\left( \frac{2}{\mu^2} - 1 \right)^2} - \sqrt{\left( \frac{2}{\mu^2} - 1 \right)^2 - 1} > 0.$$

We shall show that the derivative of  $\bar{r}$  is strictly negative for  $c_1 < c_1^-$ , whereas it is strictly positive for  $c_1 > c_1^-$ , so  $c_1^-$  is a unique minimizer. For  $c_1^- < c_1 < c_1^+$  the square-root term in (3.15) is imaginary. In this case we simply get  $\bar{r} = \sqrt{c_1}$ , whose derivative

is clearly positive. (At the endpoints  $c_1^\pm$ , where the square-root term vanishes,  $\bar{r}$  is not differentiable.) For any  $c_1 \notin [c_1^-, c_1^+]$ , the expression  $\mu(1 + c_1) + \sqrt{\mu^2(1 + c_1)^2 - 4c_1}$  is positive so we can omit the absolute value operator in (3.15) in this regime, and the derivative with respect to  $c_1$  is then given by

$$(3.17) \quad \frac{\partial \bar{r}}{\partial c_1} = \frac{1}{2} \left( \mu + \frac{\mu^2(1 + c_1) - 2}{\sqrt{\mu^2(1 + c_1)^2 - 4c_1}} \right)$$

Note that  $\frac{\mu^2(1 + c_1) - 2}{\sqrt{\mu^2(1 + c_1)^2 - 4c_1}}$  is positive for  $c_1 > \frac{2}{\mu^2} - 1$  and negative for  $c_1 < \frac{2}{\mu^2} - 1$ , hence, due to (3.16), it is positive for  $c_1^+$  and negative for  $c_1^-$ . Thus,  $\frac{\partial \bar{r}}{\partial c_1} > 0$  for  $c_1 > c_1^+$ , whereas for  $c_1 < c_1^-$  we have

$$\begin{aligned} \frac{\partial \bar{r}}{\partial c_1} &= \frac{1}{2} \left( \mu - \sqrt{\frac{(\mu^2(1 + c_1) - 2)^2}{\mu^2(1 + c_1)^2 - 4c_1}} \right) = \frac{\mu}{2} \left( 1 - \sqrt{\frac{\mu^4(1 + c_1)^2 - 4\mu^2(1 + c_1) + 4}{\mu^4(1 + c_1)^2 - 4\mu^2 c_1}} \right) \\ &= \frac{\mu}{2} \left( 1 - \sqrt{1 + \frac{4(1 - \mu^2)}{\mu^4(1 + c_1)^2 - 4\mu^2 c_1}} \right) < 0 \end{aligned}$$

The last inequality is due to the fact that that  $0 < \mu < 1$  and that  $\mu^2(1 + c_1)^2 - 4c_1 > 0$  in this regime, hence

$$\sqrt{1 + \frac{4(1 - \mu^2)}{\mu^4(1 + c_1)^2 - 4\mu^2 c_1}} > 1.$$

We thus conclude that  $\frac{\partial \bar{r}}{\partial c_1} < 0$  for  $c_1 < c_1^-$  and  $\frac{\partial \bar{r}}{\partial c_1} > 0$  for  $c_1 > c_1^-$  (with a discontinuity in the derivative at  $c_1 = c_1^+$ ), implying that the minimum is attained at  $c_1 = c_1^-$ . This completes the proof.  $\square$

To obtain the optimal convergence factor, we substitute  $c_1 = c_1^-$  into (3.15). The worst-case convergence factor with optimal  $c_1$  and  $c_2$  is then given by:

$$\bar{r} = \frac{1}{2} \mu(1 + c_1^-) = \frac{1 - \sqrt{1 - \mu^2}}{\mu}.$$

Recalling that  $\mu = \frac{\kappa-1}{\kappa+1}$ , we finally obtain

$$(3.18) \quad \bar{r} = \frac{1 - \sqrt{1 - \mu^2}}{\mu} = \frac{\sqrt{\kappa} - 1}{\sqrt{\kappa} + 1}.$$

We next summary the results of our analysis.

**Summary of Conclusions.** The optimal convergence factor of SESOP-TG with a single history direction, as approximated by our fixed-coefficient analysis, is given by (3.18)

$$\bar{r} = \frac{\sqrt{\kappa} - 1}{\sqrt{\kappa} + 1},$$

where  $\kappa$  is the condition number of  $\mathbf{W}_\alpha$ , optimized over  $\alpha \in (0, 1]$ . This is discussed further below. The optimal coefficient for the history term is given by (3.16) after simplification as

$$(3.19) \quad \bar{c}_1 = \left( \frac{\sqrt{\kappa} - 1}{\sqrt{\kappa} + 1} \right)^2,$$

which is equivalent to the square of the optimal convergence factor indicating that the usage of history will become significant if the problem is ill-posed. The optimal coefficient for the preconditioned gradient terms is given by (3.14) after simplification as

$$(3.20) \quad \bar{c}_{23} = \frac{4}{\lambda_{\min}(\sqrt{\kappa} + 1)^2}.$$

These values also apply to classical SESOP without the coarse-grid correction direction, if we select  $\alpha = 1$  rather than the  $\alpha$  which minimizes the spectral radius of  $\mathbf{W}_\alpha$ . Finally, the optimal convergence factor for SESOP-TG without the history direction is obtained by setting  $c_1 = 0$ . This yields

$$(3.21) \quad \bar{r} = \frac{\kappa - 1}{\kappa + 1},$$

with the optimal  $c_{23}$  given by

$$(3.22) \quad \bar{c}_{23} = \frac{2}{\lambda_{\min}(\kappa + 1)}.$$

Note the significant improvement provided by the use of history, with the condition number replaced by the square root. These results are reminiscent of the Conjugate Gradients (CG) method, and indeed there is an equivalence between SESOP and CG for the case of single history and no coarse-grid direction.<sup>1</sup> The advantage of SESOP is in allowing the addition of various directions. The cost is in the requirement to optimize the coefficients. This study is partly aimed at reducing this cost.

**3.1.2. Optimizing the condition number.** The upshot of our analysis thus far is that we should aim to minimize  $\kappa$ , the condition number of  $\mathbf{W}_\alpha$ . In certain cases, particularly when  $\mathbf{A}$  is a circulant matrix (typically the discretization of an elliptic partial differential equation with constant coefficients on a rectangular or infinite domain), this can be done by means of Fourier analysis. Here we begin with a more general discussion to gain insight into this matter. We consider the case of Galerkin coarsening,  $\mathbf{A}_H = (\mathbf{I}_H^h)^\top \mathbf{A} \mathbf{I}_H^h$  and no preconditioning, i.e.,  $\Phi = \mathbf{I}$ . Following ideas of [5], we assume that the columns of the prolongation matrix  $\mathbf{I}_H^h$  are comprised of a subset of the eigenvectors of  $\mathbf{A}$ .

**LEMMA 3.6.** *Let  $\eta_i$ ,  $i = 1, \dots, N$ , denote the eigenvalues of  $\mathbf{A}$ , and let  $\mathbf{w}_i$  denote the corresponding eigenvectors. Assume that the columns of the prolongation matrix  $\mathbf{I}_H^h$  are comprised of a subset of the eigenvectors of  $\mathbf{A}$ , and denote by  $\mathcal{R}(\mathbf{I}_H^h)$  the range of the prolongation, that is, the subspace spanned by the columns of  $\mathbf{I}_H^h$ . Denote*

$$\begin{aligned} \eta_{f\max} &= \max_{i: \mathbf{w}_i \notin \mathcal{R}(\mathbf{I}_H^h)} \eta_i, & \eta_{f\min} &= \min_{i: \mathbf{w}_i \notin \mathcal{R}(\mathbf{I}_H^h)} \eta_i, \\ \eta_{c\max} &= \max_{i: \mathbf{w}_i \in \mathcal{R}(\mathbf{I}_H^h)} \eta_i, & \eta_{c\min} &= \min_{i: \mathbf{w}_i \in \mathcal{R}(\mathbf{I}_H^h)} \eta_i. \end{aligned}$$

Then, the condition number of  $\mathbf{W}_\alpha$  in (3.10) with  $\Phi = \mathbf{I}$  is given by

$$(3.23) \quad \kappa = \frac{\max(\alpha\eta_{f\max}, \alpha\eta_{c\max} + 1 - \alpha)}{\min(\alpha\eta_{f\min}, \alpha\eta_{c\min} + 1 - \alpha)}.$$

---

<sup>1</sup>Note that the condition number in our scheme is specified by matrix  $\mathbf{W}_\alpha$  not  $\mathbf{A}$  which differs from the case when we do not involve the coarse correction direction.

*Proof.* Any eigenvector  $\mathbf{w}_i \in R(\mathbf{I}_H^h)$  (respectively,  $\mathbf{w}_i \notin \mathcal{R}(\mathbf{I}_H^h)$ ) is an eigenvector of the coarse-grid correction matrix  $\mathbf{I}_H^h \mathbf{A}_H^{-1} (\mathbf{I}_H^h)^T \mathbf{A}$ , with eigenvalue 1 (respectively, 0), because if  $\mathbf{w}_i \in \mathcal{R}(\mathbf{I}_H^h)$  then it can be written as  $\mathbf{w}_i = \mathbf{I}_H^h \mathbf{e}_j$  (that is, it is the  $j$ th column for some  $j$ ), so

$$[\mathbf{I}_H^h \mathbf{A}_H^{-1} (\mathbf{I}_H^h)^T \mathbf{A}] \mathbf{w}_i = \mathbf{I}_H^h [( \mathbf{I}_H^h )^T \mathbf{A} \mathbf{I}_H^h]^{-1} [( \mathbf{I}_H^h )^T \mathbf{A} \mathbf{I}_H^h] \mathbf{e}_j = \mathbf{I}_H^h \mathbf{e}_j = \mathbf{w}_i,$$

whereas if  $\mathbf{w}_i \notin \mathcal{R}(\mathbf{I}_H^h)$  then it is orthogonal to the columns of  $\mathbf{I}_H^h$ , so

$$[\mathbf{I}_H^h \mathbf{A}_H^{-1} (\mathbf{I}_H^h)^T \mathbf{A}] \mathbf{w}_i = [\mathbf{I}_H^h \mathbf{A}_H^{-1} (\mathbf{I}_H^h)^T] \eta_i \mathbf{w}_i = 0.$$

It follows that the eigenvectors of  $\mathbf{W}_\alpha$  are  $\mathbf{w}_i$ , with eigenvalues given by

$$\lambda_i = \begin{cases} \alpha \eta_i + 1 - \alpha & \text{if } \mathbf{w}_i \in \mathcal{R}(\mathbf{I}_H^h), \\ \alpha \eta_i & \text{otherwise} \end{cases}$$

The proof follows.  $\square$

We see that the second term in  $\mathbf{W}_\alpha$ , which corresponds to the direction given by the coarse-grid correction, increases the eigenvalues associated with the columns of the prolongation by  $1 - \alpha$ . It thus follows from (3.23) that, to obtain any advantage at all from the coarse-grid direction in reducing  $\kappa$ , the eigenvector associated with the smallest  $\eta_i$  must be included amongst the columns of the prolongation, and therefore  $\eta_{cmin} \leq \eta_{fmin}$ . Similarly, considering the numerator in (3.23), it is clearly advantageous that the eigenvector corresponding to the largest  $\eta_i$  not be included in the range of the prolongation. With these assumptions, we can make the following observation.

**THEOREM 3.7.** *Assume  $\eta_{cmin} \leq \eta_{fmin}$  and  $\eta_{cmax} \leq \eta_{fmax}$ . Then the condition number  $\kappa$  is minimized for*

$$\alpha = \alpha_{opt} = \frac{1}{1 + \eta_{fmin} - \eta_{cmin}} \leq 1,$$

and the resulting optimal  $\kappa$  is given by

$$(3.24) \quad \kappa = \kappa_{opt} = \begin{cases} \frac{\eta_{fmax}}{\eta_{fmin}} & \text{if } \eta_{fmax} - \eta_{fmin} \geq \eta_{cmax} - \eta_{cmin}, \\ 1 + \frac{\eta_{cmax} - \eta_{cmin}}{\eta_{fmin}} & \text{otherwise} \end{cases}$$

*Proof.* Note that  $\alpha_{opt}$  is nothing but the value of  $\alpha$  for which  $\alpha \eta_{fmin} = \alpha \eta_{cmin} + 1 - \alpha$  in the denominator in (3.23). Denote also by  $\alpha_{top} = \frac{1}{1 + \eta_{fmax} - \eta_{cmax}} \leq 1$  the value of  $\alpha$  for which  $\alpha \eta_{fmax} = \alpha \eta_{cmax} + 1 - \alpha$  in the numerator in (3.23). It is evident from (3.23) that  $\kappa$  is bounded from below by  $\eta_{fmax}/\eta_{fmin}$ . This bound can be realized when  $\eta_{fmax} - \eta_{fmin} \geq \eta_{cmax} - \eta_{cmin}$ . In this case,  $\alpha_{top} \leq \alpha_{opt}$ , and the bound is realized by selecting any  $\alpha$  in the range  $\alpha \in [\alpha_{top}, \alpha_{opt}]$ , because the numerator is then maximized by  $\alpha \eta_{fmax}$ , while the denominator is minimized by  $\alpha \eta_{fmin}$ .

When  $\eta_{fmax} - \eta_{fmin} < \eta_{cmax} - \eta_{cmin}$ , we can no longer match the lower bound. In this case  $\alpha_{top} > \alpha_{opt}$  and we have three regimes:

1.  $0 < \alpha < \alpha_{opt} \Rightarrow \kappa = \frac{\alpha \eta_{cmax} + 1 - \alpha}{\alpha \eta_{fmin}}, \frac{d\kappa}{d\alpha} = -\frac{1}{\alpha^2 \eta_{fmin}} < 0.$
2.  $\alpha_{opt} < \alpha < \alpha_{top} \Rightarrow \kappa = \frac{\alpha \eta_{cmax} + 1 - \alpha}{\alpha \eta_{cmin} + 1 - \alpha}, \frac{d\kappa}{d\alpha} = \frac{\eta_{cmax} - \eta_{cmin}}{(\alpha \eta_{cmin} + 1 - \alpha)^2} > 0.$
3.  $\alpha_{top} < \alpha < 1 \Rightarrow \kappa = \frac{\alpha \eta_{fmax}}{\alpha \eta_{cmin} + 1 - \alpha}, \frac{d\kappa}{d\alpha} = \frac{\eta_{fmax}}{(\alpha \eta_{cmin} + 1 - \alpha)^2} > 0.$

We find that  $\kappa$  decreases monotonically for  $\alpha < \alpha_{opt}$  and increases monotonically for  $\alpha > \alpha_{opt}$ , so  $\alpha_{opt}$  is indeed the minimizer. Substitution into (3.23) completes the proof.  $\square$

**Discussion.** Examining (3.24), we find that  $\kappa_{opt}$  is either equal to  $\eta_{fmax}/\eta_{fmin}$ , or else it is only “slightly larger”, because

$$1 + \frac{\eta_{cmax} - \eta_{cmin}}{\eta_{fmin}} = \frac{\eta_{fmax}}{\eta_{fmin}} + 1 - \frac{\eta_{fmax} - \eta_{cmax} + \eta_{cmin}}{\eta_{fmin}} < \frac{\eta_{fmax}}{\eta_{fmin}} + 1.$$

That is, even in the regime  $\eta_{fmax} - \eta_{fmin} < \eta_{cmax} - \eta_{cmin}$ , the optimal condition number  $\kappa_{opt}$  is increased by less than 1. Observe that  $\kappa = \eta_{fmax}/\eta_{fmin}$  yields a convergence factor (with no history) of  $\mu = \frac{\kappa-1}{\kappa+1}$ , which matches that of the classical Two-Grid algorithm with optimally weighted Richardson relaxation followed by coarse-grid correction. Indeed, our numerical tests with a variety of problems and algorithm details usually show a good agreement between SESOP-TG with no history and the classical Two-Grid algorithm with optimal weighting of the relaxation and coarse-grid correction. Of course, adding history improves the convergence rates. Finally, observe that the optimal prolongation is obtained by choosing the columns of  $I_H^h$  to be the eigenvectors associated with the smallest eigenvalues of  $\mathbf{A}$  (similarly to the classical Two-Grid case [5]). This clearly minimizes the ratio  $\eta_{fmax}/\eta_{fmin}$ . Furthermore, this choice yields  $\eta_{cmax} \leq \eta_{fmin}$ , so even if  $\eta_{fmax} - \eta_{fmin} < \eta_{cmax} - \eta_{cmin}$  (so  $\kappa_{opt} > \eta_{fmax}/\eta_{fmin}$ ), we obtain  $\kappa_{opt} = 1 + \frac{\eta_{cmax} - \eta_{cmin}}{\eta_{fmin}} < 2$ .

**3.1.3. Fourier Analysis.** In cases where  $\mathbf{A}$  is circulant, particularly discretizations of elliptic operators with constant coefficients, Fourier Analysis is a very useful quantitative tool that we can exploit [1]. Denote  $L_h$  by the elliptic operator with equal mesh size  $h$ . The grid functions  $\psi(\boldsymbol{\theta}, x, y) = e^{i\theta_1 x/h} e^{i\theta_2 y/h}$  with  $\boldsymbol{\theta} = (\theta_1, \theta_2) \in [-\pi, \pi)^2$  and  $i = \sqrt{-1}$  are the eigenfunctions of  $L_h$ , i.e.,  $L_h \psi(\boldsymbol{\theta}, x, y) = \tilde{L}_h(\boldsymbol{\theta}) \psi(\boldsymbol{\theta}, x, y)$  with  $\tilde{L}_h(\boldsymbol{\theta}) = \sum_k a_k e^{i\theta_k h}$  and  $\tilde{L}_h(\boldsymbol{\theta})$  is called the formal eigenvalue or the symbol of  $L_h$ .<sup>2</sup>  $\{a_k\}$  are the corresponding constant coefficients in  $L_h$ . Clearly, all of the grid function consists of the eigenvectors of  $\mathbf{A}$  and the eigenvalues of  $\mathbf{A}$  are specified by  $\tilde{L}_h(\boldsymbol{\theta})$ . Given the definitions of high and low frequencies in Definition 3.8, an ideal MG method should be developed to eliminate the high frequency components efficiently on fine grid and smooth the low frequency components on the coarse grid. Combining with the results shown in Lemma 3.6 and Theorem 3.7, we know that an ideal MG method should yield  $\eta_{fmax} = \max_{\boldsymbol{\theta} \in T^{high}} \tilde{L}_h(\boldsymbol{\theta})$  and  $\eta_{fmin} = \min_{\boldsymbol{\theta} \in T^{high}} \tilde{L}_h(\boldsymbol{\theta})$  and then we can simplistically estimate the  $\kappa_{opt}$  resulting in the ideal convergence rate, i.e.,  $\frac{\sqrt{\kappa_{opt}}-1}{\sqrt{\kappa_{opt}}+1}$ . In the following experiments, we will see such an ideal convergence rate is achievable.

DEFINITION 3.8 (low and high frequencies).

$$\begin{aligned} \tilde{L}_h(\boldsymbol{\theta}) \text{ is low frequency component} &\iff \boldsymbol{\theta} \in T^{low} := \left[-\frac{\pi}{2}, \frac{\pi}{2}\right)^2, \\ \tilde{L}_h(\boldsymbol{\theta}) \text{ is high frequency component} &\iff \boldsymbol{\theta} \in T^{high} := [-\pi, \pi)^2 \setminus \left[-\frac{\pi}{2}, \frac{\pi}{2}\right)^2. \end{aligned}$$

**The connection with  $h$ -ellipticity measure.**  $h$ -ellipticity measure,  $E_h(L_h)$ , is a quantitative measure of ellipticity of the discrete operator and it is defined in Definition 3.9 [14]. For an ill-posed problem, an ideal MG method should yield  $\kappa_{opt} = \frac{1}{E_h}$ . Representing the ideal convergence factor with the  $h$ -ellipticity measure of our scheme yields  $r = \frac{1-\sqrt{E_h}}{1+\sqrt{E_h}}$ . Typically, if using history is not allowed, the convergence rate becomes  $\frac{1-E_h}{1+E_h}$  which is the well known rate for the case when the optimally damped Jacobi method is chosen as the relaxation [14]. Clearly, a large  $E_h$  yields a fast convergence speed.

<sup>2</sup>Without loss of generality, we consider two dimensional cases here.

DEFINITION 3.9. *The  $h$ -ellipticity measure  $E_h$  of  $L_h$  is defined as*

$$E_h(L_h) := \frac{\min\{|\tilde{L}_h(\boldsymbol{\theta})| : \boldsymbol{\theta} \in T^{high}\}}{\max\{|\tilde{L}_h(\boldsymbol{\theta})| : \boldsymbol{\theta} \in T^{high}\}}$$

where  $\tilde{L}_h(\boldsymbol{\theta})$  represents the Fourier symbol of  $L_h$ .

**3.2. Multilevel version – SESOP-MG.** To obtain the coarse correction direction in the finest level cheaply, we suggest solving the coarse problem recursively yielding a multilevel version of our scheme named SESOP-MG. SESOP-MG is obtained via replacing Step 4 in [Algorithm 3.1](#) by [Algorithm 3.2](#). For simplicity, we only show the formulation of V-Cycle for solving the coarse problem. However, one can also easily utilize other cycles with our scheme, e.g., W-Cycle and FMG-Cycle, to improve the accuracy of the coarse solution [\[3\]](#). In practice, we can recur to one FMG-Cycle to obtain a good initial value and then call V-Cycle to save the whole computations. However, we just utilize random initialization in our experiments.

---

**Algorithm 3.2** SESOP-MG: V-Cycle

---

```

1: function  $\mathbf{x}_l^* = \dots$ 
2:   SESOP_MG_VCycle( $\mathbf{x}_{l,k}, \nabla \sigma_{l-1,k}(\mathbf{x}_{l-1,k}), L, v_1, v_2$ ) %  $l > 1$ .
3:    $\mathbf{x}_{l,k} \leftarrow \text{Relaxation}(\mathbf{x}_{l,k}, v_1)$  % Pre-relaxation
4:   Construct  $\sigma_{l,k}(\mathbf{x}_l) = f_{l,k}(\mathbf{x}_l) - \mathbf{v}_{l,k}^T \mathbf{x}_l$  where  $\mathbf{v}_l = \nabla f_{l,k}(\mathbf{x}_{l,k}) - I_h^H \nabla \sigma_{l-1,k}(\mathbf{x}_{l-1,k})$ 
5:   Calculate  $\nabla \sigma_{l,k}(\mathbf{x}_{l,k})$  and formulate the subspace
    $\mathbf{P}_k \leftarrow \nabla \sigma_{l,k}(\mathbf{x}_{l,k})$ 
5:   if  $l < L$  then
6:      $\mathbf{x}_{l+1,k} \leftarrow I_h^H \mathbf{x}_{l,k}$ 
7:     % Solve  $(l+1)$ th level problem through recursive
8:      $\mathbf{x}_{l+1}^* = \text{SESOP\_MG\_VCycle}(\mathbf{x}_{l+1,k}, \nabla \sigma_{l,k}(\mathbf{x}_{l,k}), L, v_1, v_2)$ 
9:     % add coarse correction into the subspace
10:    Formulate the coarse correction  $I_H^h(\mathbf{x}_{l+1}^* - \mathbf{x}_{l+1,k})$  and renew subspace
     $\bar{\mathbf{P}}_k \leftarrow [I_H^h(\mathbf{x}_{l+1}^* - \mathbf{x}_{l+1,k}) \quad \mathbf{P}_k]$ .
11:   else
12:      $\bar{\mathbf{P}}_k \leftarrow \mathbf{P}_k$ 
13:   end if
14:   Solve  $\boldsymbol{\alpha}_k = \text{argmin}_{\boldsymbol{\alpha}} \sigma_{l,k}(\mathbf{x}_{l,k} + \bar{\mathbf{P}}_k \boldsymbol{\alpha})$  and then  $\mathbf{x}_{l,k} \leftarrow \mathbf{x}_{l,k} + \bar{\mathbf{P}}_k \boldsymbol{\alpha}_k$ 
15:    $\mathbf{x}_{l,k} \leftarrow \text{Relaxation}(\mathbf{x}_{l,k}, v_2)$  % Post-relaxation
16: return  $\mathbf{x}_l^* \leftarrow \mathbf{x}_{l,k}$ 

```

---

**4. Experimental results.** We investigate the performance of our approach for solving linear and nonlinear test problems in this section. For the linear test problem, we mainly focus on the rotated anisotropic diffusion problem. To clearly demonstrate the potential of the proposed approach and investigate whether the above-mentioned theoretic analyses coincide with practical cases, we apply our scheme to a two-level setting for the linear problem, that is to say the hierarchy is comprised of only two-level: the original problem and just one coarser-level. For the nonlinear problems, we apply the multilevel version of our method to investigating its performance further. Moreover, we also compare our approach with steepest descent (SD), Nesterov's acceleration method [\[10\]](#) and limited-memory BFGS (LBFGS) [\[16\]](#) for solving the nonlinear problems. Moreover, denote "MG" by the classical method that exploits a

line search method to find a suitable step size for the coarse correction and does not use any history.

**4.1. Solving the rotated anisotropic diffusion problem.** The rotated anisotropic diffusion problem is described as follows:

$$(4.1) \quad \mathcal{L}\mathbf{u} = \mathbf{b},$$

where  $\mathcal{L}\mathbf{u} = \mathbf{u}_{ss} + \epsilon\mathbf{u}_{tt}$ , with  $\mathbf{u}_{ss}$  and  $\mathbf{u}_{tt}$  denoting the second partial derivatives of  $\mathbf{u}$  in the  $(s, t)$  coordinate system. Representing (4.1) in the  $(x, y)$  coordinate system, this leads

$$(4.2) \quad \mathcal{L}\mathbf{u} = (C^2 + \epsilon S^2)\mathbf{u}_{xx} + 2(1 - \epsilon)CS\mathbf{u}_{xy} + (\epsilon C^2 + S^2)\mathbf{u}_{yy},$$

where  $C = \cos \phi$  and  $S = \sin \phi$  with  $\phi$  the angle between  $(s, t)$  and  $(x, y)$ . The discrete formulation of (4.2) with mesh size  $h$  is

$$(4.3) \quad \mathcal{L}^h \otimes \mathbf{u}^h = \mathbf{b}^h,$$

where  $\otimes$  denotes the convolutional operator,

$$\mathcal{L}^h = \frac{1}{h^2} \begin{bmatrix} -\frac{1}{2}(1 - \epsilon)CS & \epsilon C^2 + S^2 & \frac{1}{2}(1 - \epsilon)CS \\ C^2 + \epsilon S^2 & -2(1 + \epsilon) & C^2 + \epsilon S^2 \\ \frac{1}{2}(1 - \epsilon)CS & \epsilon C^2 + S^2 & -\frac{1}{2}(1 - \epsilon)CS \end{bmatrix},$$

and  $\mathbf{u}^h$ ,  $\mathbf{b}^h$  are the discrete forms of  $\mathbf{u}$  and  $\mathbf{b}$  on the fine grid, respectively. Note that the coarse problem is formulated through discretizing (4.1) with mesh size  $2h$ . We choose this problem to validate whether our theoretic analyses meet the practical ones. In the following, denote “SESOP-TG- $i$ ” by the SESOP-TG with  $i$  histories and “TG” means the two-grid method with one single optimally damped Jacobi relaxation and the coarse-grid correction.

We choose a series of fixed step sizes to enforce the convergence of SESOP-TG-1.<sup>3</sup> Then, we run SESOP-TG-1 with the given step sizes until convergence and calculate the geometric average of the convergence rate at the last 10 iterations as the practical one.<sup>4</sup> We test on different  $\epsilon$  and  $\phi$  to check the accuracy of our theoretic predictions. Observing from Figure 1, we see the analytic predictions perfectly align the practical ones for various  $\epsilon$  and  $\phi$  demonstrating the accuracy of our theoretic predictions.

In the following, we choose the step sizes through solving the subspace minimization problem for SESOP-TG-1 to investigate its performance further. From Figures 2(a) and 2(c), we observe that SESOP-TG-1 converges fastest in decreasing the residual norm (defined as  $\|\mathcal{L}^h \mathbf{u}_k^h - \mathbf{b}^h\|_F$ ) than SESOP-TG-0 and TG illustrating the promising performance of our scheme. Moreover, we also compare the asymptotic convergence rate of these three methods versus cycles<sup>5</sup>, see Figures 2(b) and 2(d). Obviously, SESOP-TG-1 yields a smallest convergence factor than other two methods. Moreover, we take  $\frac{1-\sqrt{E_h}}{1+\sqrt{E_h}}$  as the ideal convergence factor to see its difference with the practical cases. From Table 1, we see the convergence factor of the practical cases meet the ideal predictions when  $\epsilon = 1$  and  $\phi = 0$ . However, for  $\epsilon = 10^{-3}$  and

<sup>3</sup>Without any confusion, We still call it SESOP-TG-1 even using fixed step sizes in this experiment.

<sup>4</sup>The convergence rate is defined as  $\frac{\|\mathcal{L}^h \mathbf{u}_{k+1}^h - \mathbf{b}^h\|_F}{\|\mathcal{L}^h \mathbf{u}_k^h - \mathbf{b}^h\|_F}$

<sup>5</sup>Without any confusion, we may also utilize iterations instead of cycles in this paper.

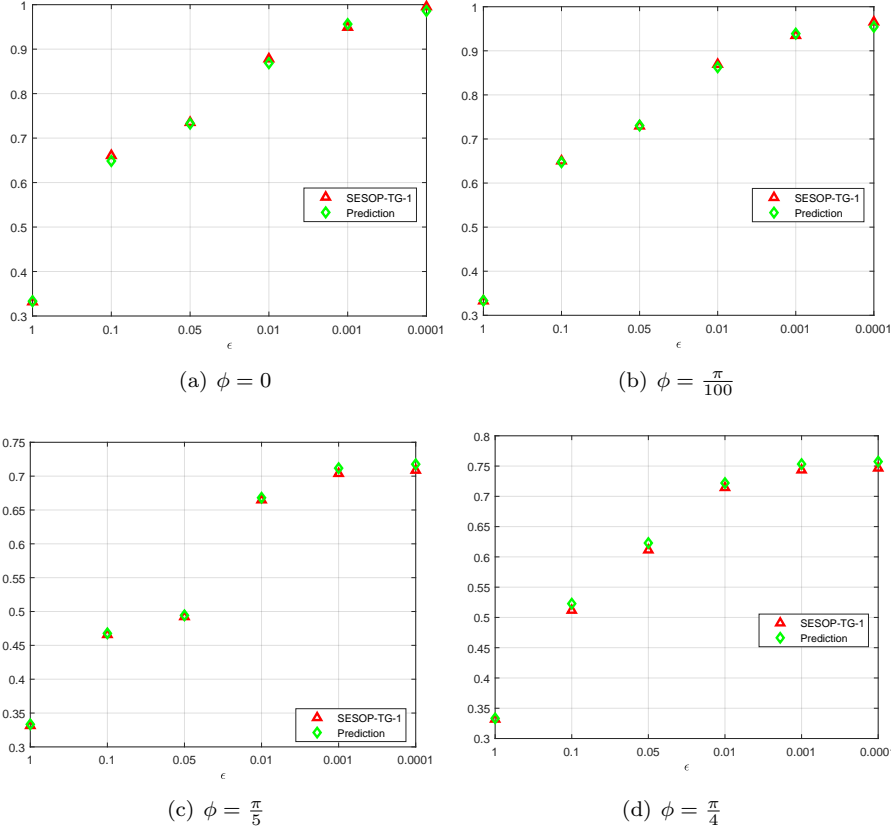


FIG. 1. The comparison of the asymptotic convergence rate between theoretic predictions and practical cases for SESOP-TG-1 with various  $\phi$  and  $\epsilon$ .

$\phi = \frac{\pi}{4}$ , the practical convergence rates become worse than the ideal one because, in general, we cannot guarantee that only high frequency is erased on the fine grid and the low frequency is smoothed on the coarse grid. Moreover, the prolongation is also not an ideal one, see Lemma 3.6 and [7].

TABLE 1

The Comparison of convergence rate between Ideal and practical cases. Left: ideal cases; right: practical cases.

$\epsilon$	$\phi$	TG	SESOP-TG-0	SESOP-TG-1
1	0	0.600	0.594	0.600
$10^{-3}$	$\frac{\pi}{4}$	0.744	0.738	0.744

Now, we utilize our theoretic analysis to see the difference of the convergence rate between the exact two-grid analysis and the ideal one. The restriction is still the full weighting, but both the bilinear and cubic prolongations are considered here to see their difference in the exact two-grid analysis. For the ordinary one, we determine the step sizes for the history and gradient by using Lemmas 3.3 to 3.5 and set the step size for the coarse correction to be 1. Moreover, we utilize a line search method to find an optimal  $\alpha$  to optimize  $\kappa$  for  $W_\alpha$  which we call the optimized one. From

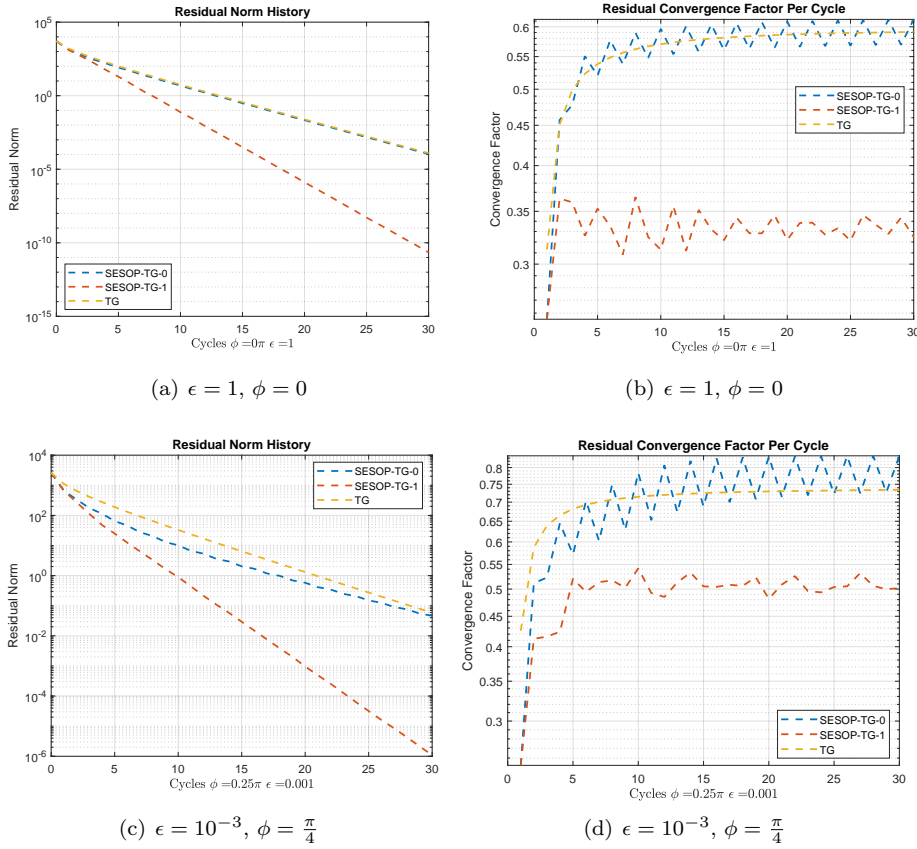


FIG. 2. Residual norm and convergence factor versus cycles with different  $\epsilon$  and  $\phi$  in the rotated anisotropic problem.

Table 2, we clearly observe that the optimized one yields a better convergence rate than the one we do not optimize  $\kappa$ . Moreover, we also see the cubic prolongation yields a better convergence rate than bilinear satisfying the expectation [7]. However, the convergence rates in the exact two-grid analysis are much worse than the ideal one if the step sizes is not well chosen when  $\phi = \frac{\pi}{4}$ . We also observe that “Opt. Bilinear” and “Opt. Cubic” yield a much better convergence rate than the ones which do not optimize the step sizes. This indicates the choice of step sizes may dominate the performance in practical situations. Interestingly, seeing Figure 2(d), SESOP-TG-1 yields a similar convergence rate with “Opt. Bilinear”, in which we choose the step sizes through optimizing  $\kappa$ . This implies the robustness of our scheme and indicates that choosing the step sizes locally can still lead to an acceptable convergence rate. Note that “Opt. Cubic” results in a similar convergence rate as the ideal one and slightly better than the ideal one in the case when  $\phi = \frac{\pi}{6}$  illustrating the effectiveness of optimizing  $\kappa$ .

**4.2. Solving Nonlinear Problems.** Two nonlinear problems are considered in this section to show the advantage of our approach for solving large-scale problems. The full weighting restriction and bilinear prolongation are chosen here. For both of the nonlinear problems, we choose the steepest descent (SD) method as the relaxation

TABLE 2

The Comparison of convergence rate between the exact two-grid analysis and Ideal ( $h$ -ellipticity measure). We utilize “Opt.” to denote the cases that utilize a line search method to optimize  $\kappa$ .

$\phi$	$\epsilon$	Bilinear	Opt. Bilinear	Cubic	Opt. Cubic	Ideal One
$\frac{\pi}{6}$	$10^{-3}$	0.673	0.581	0.588	0.569	0.587
$\frac{\pi}{6}$	$10^{-4}$	0.681	0.571	0.589	0.546	0.588
$\frac{\pi}{4}$	$10^{-3}$	0.753	0.515	0.653	0.465	0.446
$\frac{\pi}{4}$	$10^{-4}$	0.757	0.513	0.659	0.445	0.446

for MG [15] and SESOP-MG. The number of pre-relaxation and post-relaxation for MG and SESOP-MG is set to be 1 and 0, respectively. Moreover, we conduct the quasi-newton method with 10 iterations for solving the coarsest problem and the Newton method for addressing the subspace minimization problem both through the minFunc toolbox [12]. All of the experiments in this part are conducted on a work station with an Intel(R) Xeon(R) 2.20GHz CPU.

**4.2.1. Nonlinear Problem I.** We consider the following variational problem as our first nonlinear test problem,

$$(4.4) \quad \begin{cases} \min_u \mathcal{F}(u(x, y)) = \int_{\Omega} \frac{1}{2} |\nabla u(x, y)|^2 + \gamma (u(x, y)e^{u(x, y)} - e^{u(x, y)}) \\ \quad - f(x, y)u(x, y)dx dy \\ \text{such that } u = 0 \text{ on } \partial\Omega, \end{cases}$$

where  $\nabla$  is the differential operator,  $\gamma = 10$ ,  $\Omega = [0, 1] \times [0, 1]$ , and

$$f(x, y) = \left( (9\pi^2 + \gamma e^{((x^2 - x^3) \sin(3\pi y))}) (x^2 - x^3) + 6x - 2 \right) \sin(3\pi y).$$

Through the Euler-Lagrange equation, the gradient of (4.4) is

$$\nabla_u \mathcal{F} = h_x h_y (-\Delta u + \gamma u e^u - f),$$

where  $\Delta$  is the Laplacian operator,  $h_x$  and  $h_y$  denote the mesh size on the  $x$  and  $y$  axes, respectively. Moreover, the analytic solution of (4.4) with the above  $f(x, y)$  is  $u(x, y) = (x^2 - x^3) \sin(3\pi y)$  [3].

The number of grids on the finest level and the coarsest level is set to be  $1024 \times 1024$  and  $9 \times 9$ , respectively. Clearly, we have  $h_x = h_y = \frac{1}{1024}$ . Note that the equal mesh size is assumed in the this paper and denote by  $h$  for a uniform notation. The comparison of different methods for solving (4.4) is shown in Figure 3. Denote  $\mathcal{F}^*$  by the final objective value through substituting the analytic solution in (4.4). We clearly observe that SESOP-MG-1 yields the fastest convergence speed compared with other methods in terms of iteration number and CPU time illustrating the significance of involving the history. Moreover, we note that SD, Nesterov and LBFGS converge fast at the beginning of iterations but become slowly soon because they cannot eliminate the low frequency error efficiently demonstrating the potentiality of involving the coarse correction direction in our scheme.

**4.2.2. Nonlinear Problem II.** We take the following problem (called  $p$ -Laplacian) to investigate the performance of our approach further:

$$(4.5) \quad \begin{cases} \min_u \mathcal{F}(u(x, y)) = \int_{\Omega} \|\nabla u(x, y) + \xi\|^p - f(x, y)u(x, y)dx dy \\ \text{such that } u = 0 \text{ on } \partial\Omega, \end{cases}$$

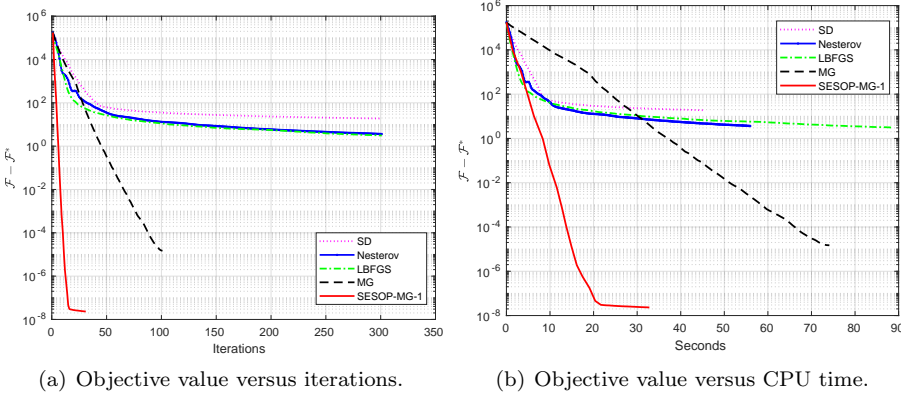


FIG. 3. The comparison of different methods for solving (4.4) with  $1024 \times 1024$  grids.

where  $p > 1$ .<sup>6</sup> The corresponding partial differential equation (PDE) of (4.5) is:

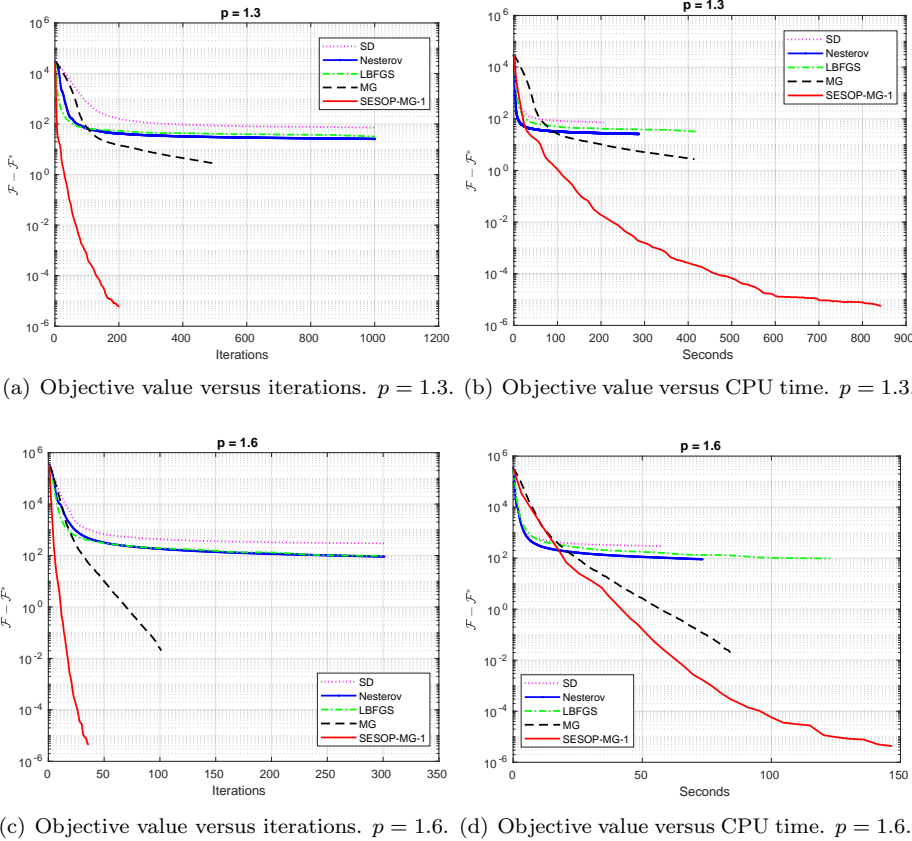
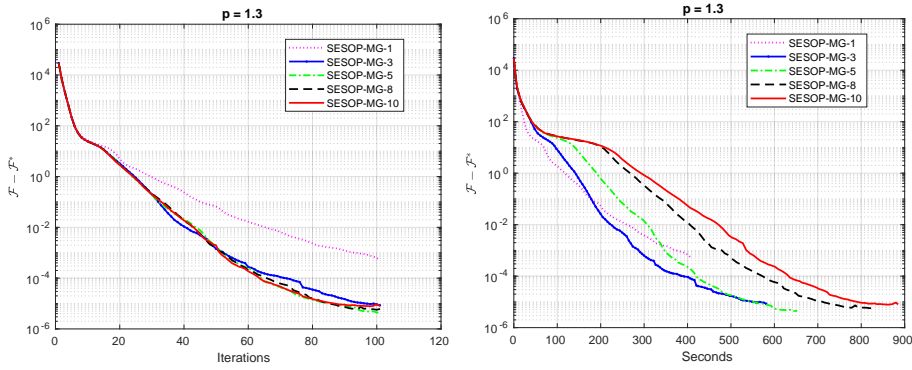
$$(4.6) \quad \begin{cases} -\nabla \cdot (\|\nabla u + \xi\|^{p-2} \nabla u) = f & \text{in } \Omega \\ u = 0 & \text{on } \partial\Omega. \end{cases}$$

The parameter  $\xi > 0$  is used as a regularization to avoid trivial value in the denominator part. We set the true  $u(x, y)$  to be  $(x^2 - x^3) \sin(3\pi y)$  and obtain  $f(x, y)$  by substituting the true  $u(x, y)$  into (4.6). Denote  $\mathcal{F}^*$  as the final objective value by substituting the true  $u(x, y)$  and corresponding  $f(x, y)$  in (4.5). We note that solving (4.5) becomes challenge if  $p$  is close to 1 and relatively easy if  $p$  is close to 2. We choose two different  $p$  to test the performance of our approach, i.e.,  $p = 1.3$  and  $1.6$ . The corresponding results are shown in Figure 4. Clearly, we observe SESOP-MG-1 outperforms other methods in terms of iterations and CPU time in both cases. We note that other methods converge fast at the beginning of iterations but become slow soon which is the same as we observed from solving (4.4) illustrating the benefit of adding the coarse direction to eliminate the smooth error.

**Investing the Influence of Using Different Number of Histories.** Now, we discuss the influence of choosing different size of histories for our approach. We apply the SESOP-MG with different size of histories to solving the  $p$ -Laplacian problem with  $p = 1.3$ . Observing from Figure 5(a), we find that adding necessary more histories can yield a faster convergence speed. However, it becomes insignificant if we add too many histories. Moreover, using more histories means more CPU time is needed to solve the subspace minimization problem. As observed in Figure 5(b), we found using three histories is a good trade-off to balance the convergence speed and the subspace minimization in this setting.

**5. Conclusions.** In this paper, we propose a novel scheme to accelerate the MG methods through SESOP for solving linear and nonlinear problems. Our idea is to merge SESOP with MG methods by adding the coarse correction direction into the subspace  $\mathbf{P}_k$  yielding a faster algorithm than the pure MG methods. The smoothing analysis for linear problems and the numerical experiments illustrate the effectiveness and robustness of our novel scheme. We hope such a novel scheme can be also used

<sup>6</sup>For simplicity, we only consider the cases when  $p < 2$  in this paper.

FIG. 4. The comparison of different methods for solving (4.5) with  $1024 \times 1024$  grids.FIG. 5. Investigating the influence of using different number of histories for solving (4.5) with  $1024 \times 1024$  grids.

to solve the large-scale problems arising in signal processing and machine learning efficiently when the hierarchy can be defined well.

## REFERENCES

- [1] A. BRANDT, *Multi-level adaptive solutions to boundary-value problems*, Mathematics of computation, 31 (1977), pp. 333–390.
- [2] A. BRANDT, *l984 multigrid guide with applications to fluid dynamics*, A. Brandt. Rigorous Local Mode Analysis of Multigrid, in Pref. Proc. SHALLOW-WATER BALANCE EQUATIONS, 25 (1985).
- [3] W. L. BRIGGS, S. F. MCCORMICK, ET AL., *A multigrid tutorial*, vol. 72, Siam, 2000.
- [4] M. ELAD, B. MATALON, AND M. ZIBULEVSKY, *Coordinate and subspace optimization methods for linear least squares with non-quadratic regularization*, Applied and Computational Harmonic Analysis, 23 (2007), pp. 346–367.
- [5] R. D. FALGOUT, P. S. VASSILEVSKI, AND L. T. ZIKATANOV, *On two-grid convergence estimates*, Numerical linear algebra with applications, 12 (2005), pp. 471–494.
- [6] S. GRATTON, A. SARTENAER, AND P. L. TOINT, *Recursive trust-region methods for multiscale nonlinear optimization*, SIAM Journal on Optimization, 19 (2008), pp. 414–444.
- [7] P. HEMKER, *On the order of prolongations and restrictions in multigrid procedures*, Journal of Computational and Applied Mathematics, 32 (1990), pp. 423–429.
- [8] G. NARKISS AND M. ZIBULEVSKY, *Sequential subspace optimization method for large-scale unconstrained problems*, Technion-IIT, Department of Electrical Engineering, 2005.
- [9] S. G. NASH, *A multigrid approach to discretized optimization problems*, Optimization Methods and Software, 14 (2000), pp. 99–116.
- [10] Y. NESTEROV, *Introductory lectures on convex optimization: A basic course*, vol. 87, Springer Science & Business Media, 2013.
- [11] C. W. OOSTERLEE AND T. WASHIO, *Krylov subspace acceleration of nonlinear multigrid with application to recirculating flows*, SIAM Journal on Scientific Computing, 21 (2000), pp. 1670–1690.
- [12] M. SCHMIDT, *minfunc: unconstrained differentiable multivariate optimization in matlab*, Software available at <http://www.cs.ubc.ca/~schmidtm/Software/minFunc.htm>, (2005).
- [13] K. STÜBEN, *An introduction to algebraic multigrid*, Multigrid, (2001), pp. 413–532.
- [14] U. TROTTERBERG, C. W. OOSTERLEE, AND A. SCHULLER, *Multigrid*, Academic press, 2000.
- [15] Z. WEN AND D. GOLDFARB, *A line search multigrid method for large-scale nonlinear optimization*, SIAM Journal on Optimization, 20 (2009), pp. 1478–1503.
- [16] S. WRIGHT AND J. NOCEDAL, *Numerical optimization*, Springer Science, 35 (1999), p. 7.
- [17] J. XU AND L. ZIKATANOV, *Algebraic multigrid methods*, Acta Numerica, 26 (2017), pp. 591–721.
- [18] M. ZIBULEVSKY, *Speeding-up convergence via sequential subspace optimization: Current state and future directions*, arXiv preprint arXiv:1401.0159, (2013).
- [19] M. ZIBULEVSKY AND M. ELAD, *L1-l2 optimization in signal and image processing*, IEEE Signal Processing Magazine, 27 (2010), pp. 76–88.